Received: 29 June 2018 | Revised: 25 September 2018 | Accepted: 16 November 2018 | Published on: 13 December 2018

DOI: 10.1002/joc.5935

International Journal of Climatology | RMetS

RESEARCH ARTICLE

The influence of atmospheric circulation patterns on cold air outbreaks in the eastern United States

Erik T. Smith | Scott C. Sheridan

Kent State University, Kent, Ohio

Correspondence
Kent State University, PO Box 5190, Kent, OH 44242.
Email: esmit149@kent.edu

In this paper, we build upon previous literature in directly addressing the temporal relationship between the stratospheric and tropospheric polar vortex (PV), sea level pressure (SLP), and resultant cold air outbreaks (CAO). An atmospheric and teleconnection analysis was conducted on 49 predefined CAOs across the eastern United States from 1948 to 2016. Clusters of SLP, 100 and 10-mb geopotential height anomalies were mapped utilizing self-organizing maps (SOMs) to understand the surface, tropospheric PV, and stratospheric PV patterns preceding CAOs. The Arctic Oscillation (AO), North Atlantic Oscillation (NAO), and Pacific–North American (PNA) teleconnections were used as variables to explain the magnitude and location of mid-latitude Arctic air displacement. Persistently negative SLP anomalies across the Arctic and North Atlantic were evident 1–2 weeks prior to the CAOs throughout the winter. The tropospheric and stratospheric PV were found to be persistently weak/weakening prior to mid-winter CAOs and predominantly strong and off-centred prior to early and late season CAOs. Negative phases of the AO and NAO were favoured prior to CAOs, while the PNA was found to be less applicable. This method of CAO and synoptic pattern characterization benefits from a continuous pattern representation and provides insight as to how specific teleconnections and atmospheric patterns lead to CAOs in the eastern United States.

KEYWORDS

climate, cold air outbreaks, extreme cold, mid-latitudes, polar vortex, self-organizing maps, synoptic climatology, teleconnections, United States

1 | INTRODUCTION

A cold air outbreak (CAO), defined as a southwards displacement of polar air over the Northern Hemisphere (Wheeler *et al.*, 2011), can have detrimental impacts on human health, agriculture, and energy consumption. Due to the severity and relatively uncommon nature of CAOs, it is vital to gain a better understanding of how these events unfold, as the evolution of atmospheric patterns preceding CAOs, along with the geographic extent of their displacement, remain poorly understood (Cellitti *et al.*, 2006). Much knowledge of the causal mechanisms of CAOs has been achieved through case studies, climate pattern analyses, and climate trend studies (Cellitti *et al.*, 2006; Vavrus *et al.*, 2006; Westby and Black, 2015).

CAOs are largely dependent on the cold air displaced from the Arctic via a circulation known as the polar vortex (PV) which exists separately in both the troposphere and stratosphere (Waugh *et al.*, 2017). While there have not been many studies statistically connecting changes in the PV to CAOs, studies from Cellitti *et al.* (2006) and Wheeler *et al.* (2011) determined that a weaker than average PV is present leading up to a CAO onset. Mitchell *et al.* (2013) found that split PV events often lead to colder temperatures across Eurasia, while displaced PV events are related to CAOs across North America. Split PV events occur more frequently during the first half of winter, with a peak in January, while displaced vortex events are skewed towards late winter (Seviour *et al*., 2013). Recent studies focused on the interaction between the troposphere and stratosphere have proven to be a valuable tool when making predictions of several weeks or more. A weakened stratospheric PV circulation often results from sudden stratospheric warmings (SSW) and manifests in the form of splits and displacements, both of which can impact the mid-latitudes with Arctic air intrusions (Mitchell *et al*., 2013). Cohen and Jones (2011) found that a SSW event can split or displace the stratospheric PV leading to extreme cold in the tropospheric mid-latitudes. It is thought that stratospheric circulation anomalies may have a lagged effect of the same sign on the troposphere (Baldwin and Dunkerton, 2001). Thus, a better understanding of stratospheric forcing mechanisms may help forecast a CAO many weeks in advance.

More broadly studied than individual atmospheric circulation features have been the large-scale patterns that are associated with anomalous weather conditions. These relationships between low-frequency circulation patterns and weather in both the atmosphere and ocean are referred to as teleconnections. The Arctic Oscillation (AO), centred in the Arctic, is the leading mode of sea level pressure (SLP) variability in the NH and is a surface representation of the PV circulation (Deser, 2000). During a negative AO, a weak PV results in a more meridional polar jet stream, allowing the displacement of Arctic air into the mid-latitudes. The trend towards a weakened AO is considered to have played a major role in the increase in the number of extreme temperature events in the northeastern United States during recent decades (Griffiths and Bradley, 2007). While the AO is typically anomalously weak during eastern U.S. CAOs, Cellitti *et al*. (2006) found very little correlation between the strength of the PV and the intensity of CAOs. However, the AO can influence the eastern United States through modulations, or phases, of the well-studied North Atlantic Oscillation (NAO; Wallace and Gutzler, 1981; Wettstein and Mearns, 2002) and Pacific–North American (PNA; Nathaniel *et al*., 2008; Ning and Bradley, 2014) pattern. For instance, a negative AO and NAO occurring simultaneously can significantly increase the likelihood of polar air displacing into the eastern United States (Pinto *et al*., 2011). A positive PNA index can contribute to the intrusion of polar air masses in the south-central United States from cyclonic circulation located across the southeastern United States (Ning and Bradley, 2014). Furthermore, Kolstad *et al*. (2010) showed that the AO could be modulated via the stratosphere; thus, the AO can be interpreted as the surface signature of modulations in the strength of the PV aloft (Thompson and Wallace, 1998).

One way to holistically evaluate atmospheric circulation is through synoptic classification. In particular, self-organizing maps (SOMs; Kohonen, 2013) can be used to diagnose climate variability by analysing many patterns as a continuum, since it uses organized nodes, rather than more randomized discrete patterns typical of other classifications (Sheridan and Lee, 2011). The continuous data can then be efficiently displayed on a two-dimensional grid, defined by the user, with the most extreme patterns typically confined to the edges of the SOM. SOMs have been used to analyse climate variability and connections in a number of studies (Cassano *et al*., 2006; Huth *et al*., 2008; Sheridan and Lee, 2011; Gibson *et al*., 2016).

In this study, we utilize SOMs to understand the preferred atmospheric patterns and teleconnection indices across the Northern Hemisphere prior to and during CAOs that occur in the eastern United States. We build upon Smith and Sheridan (2018a,b), in which CAOs were identified, by focusing on the circulation of both the tropospheric and stratospheric PV along with the SLP patterns and teleconnection patterns preceding CAOs. The uncertainties among stochastic global circulations and CAOs are addressed via three essential questions:

1. Which synoptic-scale variables are best used as precursors to CAOs across the eastern United States?
2. From these synoptic variables, which patterns occur most frequently prior to a CAO onset?
3. Do certain combinations of teleconnection phases more frequently lead to the aforementioned synoptic patterns and to CAOs?

2 | DATA AND METHODS

2.1 | Cold air outbreaks

This study utilizes the 49 CAOs defined by Smith and Sheridan (2018a,b) from November 1948 through March 2016 for 20 surface weather stations in the eastern United States (Table 1). The CAOs in this data set were based on a set of criteria concerning duration, spatial extent, and magnitude and are listed below (Smith and Sheridan, 2018a,b):

1. The daily maximum and minimum temperatures must be at least 1.25σ below the 67-year daily climatological mean.
2. The duration must be at least 5 days in which the daily maximum and minimum temperatures are at least 1.25σ below the climatological mean.
3. Three contiguous surface stations must simultaneously meet the magnitude and duration criteria.

2.2 | Atmospheric patterns

To categorize Arctic circulation, daily mean geopotential height at 100 mb (100z) and 10 mb (10z), along with SLP were acquired for 45°–90°N and 0°–357.5°W from the National Centers for Environmental Prediction (NCEP) Reanalysis Project (Kalnay *et al*., 1996) from 1948 to 2016.

TABLE 1 Surface weather stations. Replacement stations were used to fill the 347 missing days for the Saline Area station

Weather station	WBAN number	FAA location ID	Missing days	Replacement station
Atlanta, Georgia	13874	ATL	0	
Boston, Massachusetts	14739	BOS	0	
Buffalo, New York	14733	BUF	1	
Chicago, Illinois	Chicago Area	Chicago Area	0	
Cincinnati, Ohio	93814	CVG	1	
Dallas, Texas	13960	DAL	30	
Des Moines, Iowa	14933	DSM	0	
Detroit, Michigan	Detroit Area	Detroit Area	0	
Little Rock, Arkansas	13963	LIT	0	
Miami, Florida	12839	MIA	0	
Minneapolis, Minnesota	14922	MSP	0	
Nashville, Tennessee	13897	BNA	0	
New Orleans, Louisiana	12916	MSY	0	
Oklahoma City, Oklahoma	13967	OKC	5	
Orlando, Florida	Orlando Area	Orlando Area	3	
Philadelphia, Pennsylvania	13739	PHL	0	
Pierre, South Dakota	24025	PIR	28	
Raleigh, North Carolina	13722	RDU	0	
Salina, Kansas	Salina Area	Salina Area	347	Abilene, Kansas and McPherson, Kansas
St. Louis, Missouri	13994	STL	0	

The data spans October through March as the focus is on the cold season. Anomalies relative to the time of year for 10z, 100z, and SLP were chosen because they had much less seasonality than the raw data. The anomalies were calculated by subtracting the daily values from the 30 year (1981–2010) 7 day centred moving average, in which the centred moving average was calculated after the 30 year average. A 7 day centred moving average was used to limit the effects of extreme data points. While other variables were considered, in preliminary examinations, these three variables had more statistically significant results than the other variables such as zonal wind. SLP was used for the surface pattern analysis of the Arctic and better depicted the atmospheric conditions near the CAO onset as opposed to the lower variability 10z and 100z anomalies. Since the PV exists as two separate circulations, 10z anomalies were used for the stratospheric PV, while the 100z anomalies were used as an intermediate layer (tropopause) to better understand the relationship between the stratospheric and tropospheric PV as it manifests near the tropopause.

As much of the analysis is focused upon units of weeks, to evaluate seasonality the winter was divided into five 28-day (4 week) periods (Table 2), with period 1 (P1) beginning on November 1 and P5 ending on March 23, the last onset day of the latest CAO for the study period. SOM nodes for the 28 days preceding each CAO onset were analysed in weekly frequencies (W1, the week before, to W4, four weeks before) to better understand the progression of specific patterns leading up to the CAO onset. Along with the SOM patterns present during the CAO onset through Day 5 of the CAO.

TABLE 2 Twenty-eight-day periods of the winter season

Period	Calendar dates	Number of CAOs
P1	Nov 1–Nov 28	6
P2	Nov 29–Dec 26	12
P3	Dec 27–Jan 24	16
P4	Jan 25–Feb 22	9
P5	Feb 23–Mar 23	6

Ratios were then used to quantify the synoptic pattern frequencies of occurrence prior to the CAO onset, for each of the five periods (P1–P5). The ratio was determined by dividing the percentage a pattern occurred during each of the 4 weeks prior to a CAO onset (W4–W1) with the percentage that the pattern was expected to occur climatologically. The climatological value was calculated according to the day-of-season (DOS) value between 1 and 182 (October 1 through March 31), excluding all February 29th days during leap years. The percentage of occurrence of each pattern on each DOS was determined for the full period, and a 7-day moving average frequency was then calculated to smooth out day-to-day fluctuations. By using each CAO's onset date, the climatologically expected occurrence of each pattern present *n*-days before a CAO onset could be determined and grouped according to the period (graph to the left of SOM pattern in Figures 1–3). Significance levels were calculated using a difference of proportions z-test (Ott, 1977) for the 0.05 ($z = 1.65$) and 0.10 ($z = 1.96$) confidence levels for each ratio based on the sample size of the data.

This study utilizes 3×3 SOMs, or nine nodes, to display the clusters of SLP and geopotential height patterns

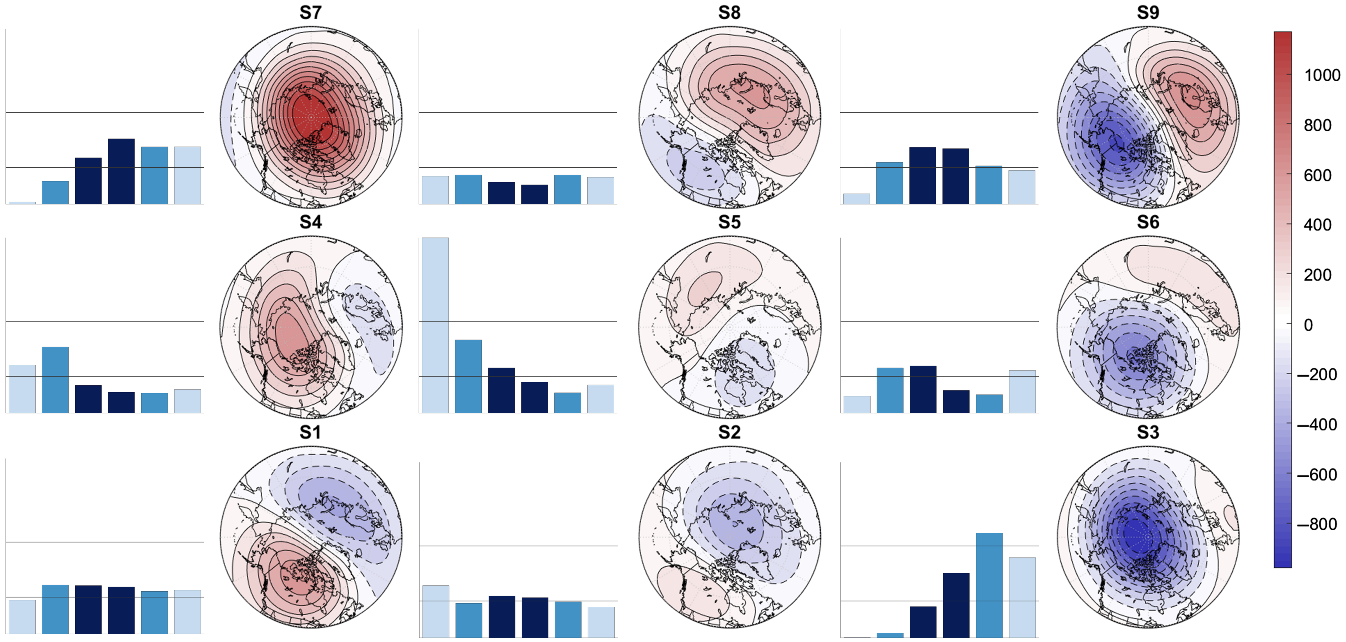

FIGURE 1 10za (10-mb geopotential height anomalies) SOM from 45°N to 90°N where the red shading (solid lines) represents anomalously high geopotential heights and blue (dashed lines) represents anomalously low geopotential heights. The bar graph to the left of each SOM represents the adjacent patterns seasonality, where the *y*-axis is the percentage of pattern occurrences per period (bottom grey line = 10%, top grey line = 25%) and the *x*-axis is the six 28-day atmospheric periods, beginning October 4 through March 21 [Colour figure can be viewed at wileyonlinelibrary.com]

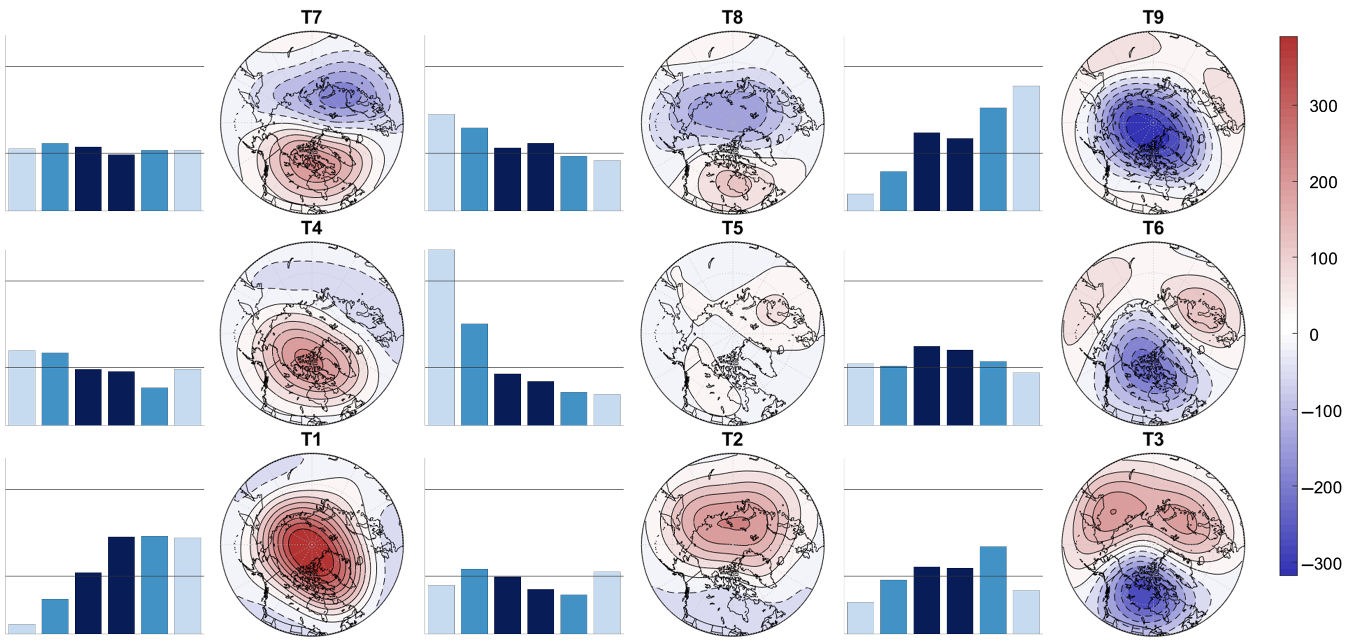

FIGURE 2 100za (100-mb geopotential height anomalies) SOM from 45°N to 90°N where the red shading (solid lines) represents anomalously high geopotential heights and blue (dashed lines) represents anomalously low geopotential heights. The bar graph to the left of each SOM represents the adjacent patterns seasonality, where the *y*-axis is the percentage of pattern occurrences per period (bottom grey line = 10%, top grey line = 25%) and the x-axis is the six 28-day atmospheric periods, beginning October 4 through March 21 [Colour figure can be viewed at wileyonlinelibrary.com]

from 1948 to 2016. The size of the dimensions was chosen based on the orientation of the SOM in which the weight positions of the nodes were spread uniformly across the two-dimensional plane. Furthermore, the 3x3 SOMs had the best internal cluster validations for all three atmospheric variables as compared to other SOM dimensions tested. The data set was iterated 10,000 times to ensure nodes were clustered adequately. An ordering phase learning rate of 0.90 and a tuning phase learning rate of 0.02 were used to update the nodes with each iteration.

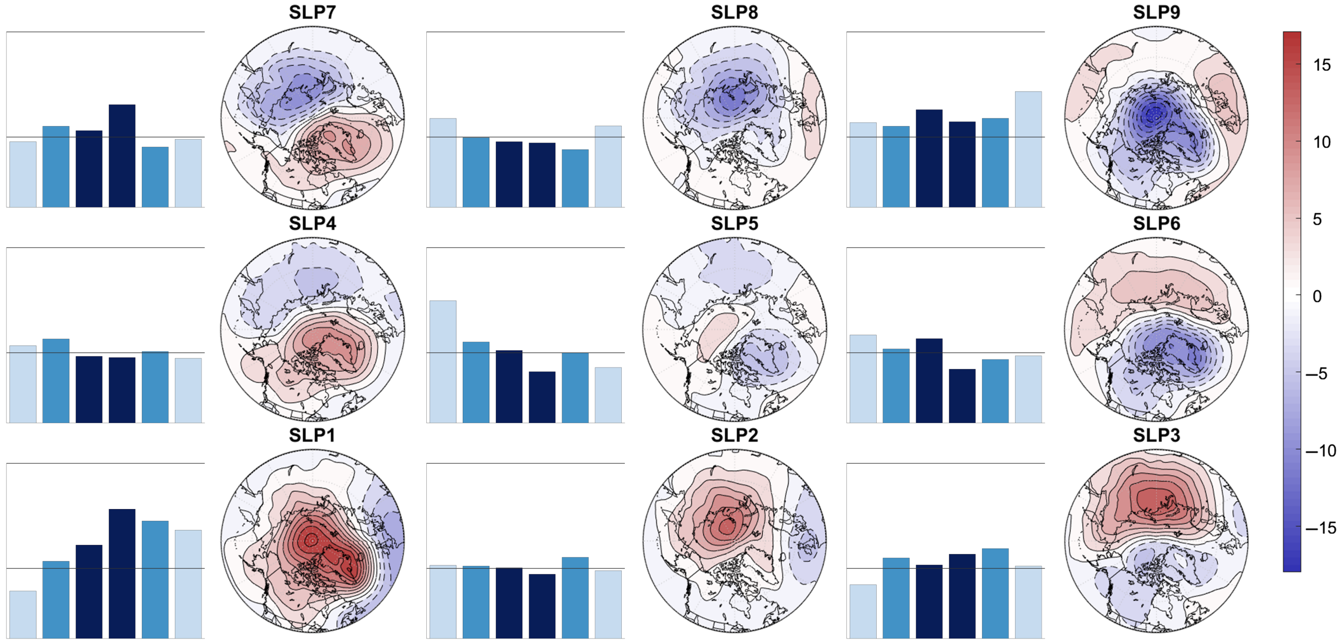

FIGURE 3 SLPa (Sea-level pressure anomalies) SOM from 45°N to 90°N where the red shading (solid lines) represents anomalously high geopotential heights and blue (dashed lines) represents anomalously low geopotential heights. The bar graph to the left of each SOM represents the adjacent patterns seasonality, where the *y*-axis is the percentage of pattern occurrences per period (bottom grey line = 10%, top grey line = 25%) and the *x*-axis is the six 28-day atmospheric periods, beginning October 4 through March 21 [Colour figure can be viewed at wileyonlinelibrary.com]

2.3 | Teleconnections

A teleconnection analysis was conducted to reinforce the findings of the synoptic variables and to better understand the atmospheric precursors to CAOs. This study uses the AO, NAO, and PNA daily normalized indices from the Climate Prediction Center (CPC) from January 1950 through March 2016. Daily indices were analysed 28 days prior to the CAO onset through Day 5 for each CAO. This approach was similar to the synoptic analysis, in which the evolution of the teleconnection indices approaching the CAO and during the CAO was evaluated. In the daily analysis, each teleconnection was composited for each SOM variable pattern (10z, 100z, and SLP anomalies) to depict the average phase per pattern. The daily indices were also analysed by period. Like the synoptic analysis, the average phase of each teleconnection was divided into 4 weeks prior to the CAO onset through Day 5 of the CAO. The monthly teleconnection indices were then averaged for the 10 most extreme CAOs in terms of duration, magnitude, and spatial extent events. Similarly, the duration, magnitude, spatial extent, and CAO days were averaged for the 10 most extreme positive and negative values of each teleconnection index. The same difference of proportions significance test used for the atmospheric variables was used to determine the significance of the teleconnection indices.

3 | RESULTS

3.1 | Atmospheric patterns

3.1.1 | Overview of SOMs

The 10za SOM (Figure 1), which represents modes of variability in the stratospheric PV, depicts an array of anomalous geopotential height patterns and are numbered with an "S" for stratosphere preceding each SOM pattern. SOM is characterized by weakened PV patterns in the upper left corner (S7) and stronger PV patterns in the lower right corner (S3). The more anomalous patterns occur infrequently early in the winter but become more common as the winter progresses. S1, S4, S7, and S8 are classified as weak PV patterns, while S2, S3, S6, and S9 are classified as strong PV patterns. The centre of the SOM (S5) represents near normal patterns, with only slightly negative height anomalies over the North Atlantic and slightly positive height anomalies over Eurasia. As S5 happens frequently during early winter but much less frequently thereafter, it can be viewed as a transitional pattern between the fall and winter season.

Geopotential heights at the 100-mb level (Figure 2) characterize the state of the upper troposphere (tropopause), thus each SOM pattern is numbered with a preceding "T." Though just above the tropospheric PV, the 100za SOM will be discussed in terms of its implications on the tropospheric PV since it exists closely to the tropospheric circulation. The 100za patterns had a higher-frequency pattern variability with more persistent patterns than the 10za SOM, but lower-frequency pattern variability than the SLP anomalies (SLPa) SOM. The 100za SOM is characterized strong PV patterns in the upper right corner (T6, T8, and T9) to weak PV patterns in the lower left corner (T1, T2, and T4). Like the 10za SOM, the centre of the SOM (T5) represents near-normal heights and occurred most frequently during the early winter; therefore, it can be viewed as a transitional pattern between the fall and winter season. T7 and T8 feature two regions of primarily negative height anomalies across the

Barents–Kara Seas, with positive height anomalies across northern Canada, indicative of an off-centred PV towards Siberia.

The SLPa SOM (Figure 3) consists of several regions of anomalous SLP and is numbered with an “SLP” preceding each SOM pattern. Positive SLP anomalies over the pole, indicative of a weaker PV, are focused on the lower left side of the SLPa SOM, while the upper right portion of the SOM consists of negative polar SLP anomalies, indicative of a stronger PV. SLP2, SLP3, SLP4, and SLP7 are variations of Arctic high-pressure patterns with shifts in the positive anomalies towards Siberia in SLP2 and SLP3 and a shift towards the North Atlantic in SLP4 and SLP7. All four patterns represent a disturbed PV with a different centroid of positive SLP anomalies. SLP5, much like the 10za and 100za SOMs, is a near-normal pattern and occurs most frequently during the beginning of the winter. However, unlike the 10za and 100za, SLP5 continues to occur relatively frequently during P2–P5. Consistency among the patterns is greatest during P2 when a transition from a predominantly zonal flow to a more meridional flow is taking place. By P3 and extending through P5, the most anomalous SLPa patterns (SLP1, SLP3, SLP7, and SLP9) occur most frequently.

3.1.2 | 10z anomalies (10za) SOM

The ratio of each 10za SOM patterns occurrence preceding the CAO onset during each of the five periods is shown in Table 3. For period 1 (P1), covering most of November, the 10za pattern that dominates 3–4 weeks before the onset of a CAO is S5 (62% in W4), unsurprising since it is the predominant pattern during October. Starting 2 weeks before a CAO, there is a clear trend towards a strengthening PV, as off-centred PV patterns (particularly S8 and S9) increased in frequency. Week 1 revealed the strongest relationship, with S9 (off-centred PV over North America) being 6.1 times (52% of all patterns) more likely to occur in the week preceding a CAO than would be expected.

Period 2 (P2) was characterized by a persistently weak PV (S1, S4, S7, and S8) preceding CAOs. Four weeks before an outbreak, S1, S4, and S7 are nearly twice as likely to occur than what is climatologically expected, accounting for 77% of all pattern occurrences. During Week 3, S7 and S8 occur twice as often as expected and account for 38% of all pattern occurrences. Weaker PV patterns are favoured during P4 and P5.

Well in advance of CAO during period 3 (P3), weak PV (S4, S7, and S8) patterns were favoured, with S4 occurring nearly 2.5 times as often as expected 3–4 weeks ahead. An off-centred, strong PV (S9) increased in frequency during Weeks 3 and 2, but returned to the climatologically expected frequency by Week 1 through the onset. In the 2 weeks before a CAO, there is no clear signal of preceding stratospheric conditions, with only slightly negative height anomalies over North America (S5) favoured post-CAO onset.

Moving into February CAOs, period 4 (P4) can be characterized by high frequencies of a strong PV transitioning to a weak PV by the CAO onset. Off-centred, strong PV patterns occurred 1.6 (S9) and 2.6 (S6) times as often as expected 4 weeks before P4 CAOs. A strong PV (S1), with positive height anomalies centred over northern Canada and negative height anomalies over the Barents–Kara Seas, occurred most frequently during Week 3. However, a weakening of the PV was evident from Week 2 through the onset with S2 and S3 favoured during Week 2 and S1, S4, and S7 increasing in frequency Week 1 through the onset.

Like P4, a strong PV occurred frequently during the period leading up to period 5 (P5) CAOs. Though not statistically significant due to the small sample size of late season CAOs, S6 is 5.1 times more likely to occur during Week 4. S3 and S6 account for 88% of all pattern occurrences during Week 4 of P5. The frequency of occurrence of a strong PV (S3) decreases through Week 2 in favour of an off-centred PV (S9) and a weaker PV (S1) which was nearly 3 times as likely to occur. By Week 1, a weakened PV occurs most frequently (S1, S2, and S5). A strong, off-centred PV over the Beaufort Sea (S6) began to remerge after the CAO onset. P5 experienced very few occurrences of weak PV patterns S4, S7, and S8.

3.1.3 | 100z anomalies (100za) SOM

The ratio of each 100za SOM patterns occurrence preceding the CAO onset during each of the five periods is shown in Table 4. Period 1 (P1) CAOs were characterized by a frequent off-centred PV across the Barents–Kara Seas (T7 and T8) and a reduction in the frequency of T5 3–4 weeks in advance of the outbreak. By Week 2, a weak PV centred over the Arctic begins to increase in frequency (T1), however, it is a strong PV over northwest Canada with positive height anomalies across Siberia (T3) that occurred most frequently during Week 2, occurring 5 times more often than expected. By Week 1, off-centred PV patterns over northern Canada and positive height anomalies across northern Eurasia were 2–3 times more likely to occur and accounted for 67% of all pattern occurrences (T2, T3, and T6). The off-centred PV patterns transition towards weak PV patterns centred over the Arctic and Beaufort Sea (T1 and T4) post-CAO onset, with T1 6 times as likely and T4 nearly 4 times as likely as expected.

Persistently weak PV patterns (T1, T4, and T7) were favoured throughout period 2 (P2). Transitional pattern T5, along with weak PV patterns T4 and T7, occurred most frequently 3–4 weeks in advance of P2 CAOs, with T7 being more than twice as likely to occur than expected. An increase in weak PV patterns T4, T5, T7, and T8 were

TABLE 3 (Top) Ratios of 10za pattern occurrences before CAOs and the climatologically expected occurrence. Blue shaded values indicate patterns which occur significantly more frequently prior to CAOs than climatologically expected, while red shaded values occur significantly less frequently prior to CAOs. Bold italic values are statistically significant, where dark blue and dark red are statistically significant at the 95% confidence level while light blue and light red are statistically significant at 90% confidence level. (Bottom) Percentage of occurrence of each pattern. Columns represent each of the five periods (P1–P5). Rows represent weeks before onset (W1–W4) and onset—day 5 of the CAO (O–D5)

Ratio	P1			P2			P3			P4			P5		
W4 Ratio	0.0	***0.0***	0.9	***2.7***	***0.5***	0.7	***1.4***	***1.8***	***0.3***	***0.6***	0.9	***1.6***	***0.0***	***0.0***	***0.0***
	0.5	***1.3***	2.1	***2.1***	***0.5***	***0.0***	***2.5***	1.1	1.0	0.6	0.6	***2.6***	***0.0***	1.6	***5.1***
	1.2	***0.5***	0.0	***1.5***	***0.0***	0.0	1.0	0.8	***0.1***	1.0	***0.4***	1.0	***0.0***	***0.2***	***1.9***
%	0%	0%	2%	17%	5%	8%	17%	11%	4%	11%	5%	24%	0%	0%	0%
	7%	62%	10%	37%	11%	0%	19%	13%	13%	3%	5%	16%	0%	10%	31%
	12%	7%	0%	23%	0%	0%	13%	9%	1%	13%	5%	19%	0%	2%	57%
W3 Ratio	0.0	0.6	***0.0***	***2.2***	***2.0***	***0.4***	***1.4***	***1.5***	***1.6***	0.9	0.5	***0.4***	***0.0***	***0.0***	1.4
	1.0	1.0	0.6	0.7	1.1	***0.1***	***2.4***	0.7	***0.5***	***0.0***	0.6	0.8	***0.0***	1.8	0.9
	2.4	0.7	0.0	***1.5***	0.6	***0.0***	***0.7***	***0.5***	***0.6***	1.0	1.0	***2.2***	***2.2***	0.7	***1.3***
%	0%	5%	0%	21%	17%	6%	19%	10%	21%	17%	3%	6%	0%	0%	12%
	17%	40%	5%	11%	19%	1%	15%	7%	4%	0%	5%	5%	0%	10%	7%
	24%	10%	0%	20%	5%	0%	10%	6%	8%	11%	10%	43%	26%	7%	38%
W2 Ratio	0.0	***2.3***	***3.0***	***1.5***	0.9	***1.3***	***2.2***	0.9	***1.6***	1.2	***0.0***	***0.0***	***0.0***	***0.0***	***1.8***
	0.4	1.0	0.3	***1.5***	***0.6***	0.7	0.9	***0.5***	1.0	1.5	***0.0***	1.2	1.0	***0.0***	1.1
	1.6	***0.0***	***0.0***	0.7	1.2	***0.0***	***0.4***	***0.2***	0.9	1.5	***1.7***	***1.6***	***2.9***	0.5	1.0
%	0%	19%	21%	17%	6%	21%	33%	5%	21%	22%	0%	0%	0%	0%	17%
	7%	31%	2%	18%	10%	10%	4%	4%	7%	8%	0%	6%	7%	0%	10%
	19%	0%	0%	8%	11%	0%	6%	3%	15%	14%	16%	33%	38%	5%	24%
W1 Ratio	***0.0***	***2.0***	***6.1***	1.3	***1.8***	0.8	1.3	1.4	0.8	***1.5***	***0.0***	***0.0***	***0.0***	0.7	***0.3***
	0.0	***0.4***	0.9	***2.9***	***0.1***	0.8	0.9	1.1	***1.7***	1.3	0.8	***0.3***	0.4	***2.7***	1.5
	1.3	***0.0***	0.0	1.2	0.6	***0.0***	***0.5***	***0.6***	1.1	***2.6***	1.3	0.8	***1.9***	***2.0***	***0.5***
%	0%	12%	52%	15%	11%	14%	21%	9%	12%	27%	0%	0%	0%	5%	2%
	0%	10%	10%	27%	1%	12%	4%	10%	11%	6%	5%	2%	2%	21%	17%
	17%	0%	0%	13%	6%	0%	7%	7%	20%	27%	13%	21%	24%	17%	12%
O-D5 Ratio	***0.0***	***1.8***	***2.1***	***2.1***	0.6	1.0	1.0	***0.0***	0.8	0.7	1.3	***0.0***	***0.4***	***0.0***	1.6
	0.4	***1.4***	0.8	***2.0***	***1.5***	***0.6***	1.0	***2.6***	1.0	***2.1***	***0.0***	***0.0***	0.5	***2.4***	***2.6***
	1.2	***0.0***	0.0	***0.1***	1.0	***0.0***	***0.6***	1.0	0.9	***1.8***	1.4	1.2	0.6	***0.0***	0.9
%	0%	13%	23%	25%	3%	15%	19%	0%	13%	11%	11%	0%	7%	0%	13%
	7%	30%	10%	17%	18%	8%	6%	21%	6%	11%	0%	0%	3%	17%	33%
	17%	0%	0%	2%	12%	0%	9%	10%	16%	20%	13%	33%	7%	0%	20%

TABLE 4 (Top) Ratios of 100za pattern occurrences before CAOs and the climatologically expected occurrence. Blue shaded values indicate patterns which occur significantly more frequently prior to CAOs than climatologically expected, while red shaded values occur significantly less frequently prior to CAOs. Bold italic values are statistically significant, where dark blue and dark red are statistically significant at the 95% confidence level while light blue and light red are statistically significant at 90% confidence level. (Bottom) Percentage of occurrence of each pattern. Columns represent each of the five periods (P1–P5). Rows represent weeks before onset (W1–W4) and onset—day 5 of the CAO (O–D5)

Ratio	P1			P2			P3			P4			P5		
W4	***2.0***	0.9	0.0	0.8	0.7	0.4	1.0	***0.2***	***0.2***	1.3	0.8	***1.6***	***0.0***	***0.2***	***2.0***
Ratio	0.8	1.2	1.2	***1.5***	1.3	***0.0***	***2.1***	***1.6***	***1.3***	***0.2***	0.6	0.6	***0.0***	0.8	2.6
	0.0	***0.0***	0.9	1.5	1.2	1.3	1.3	0.8	0.8	1.1	***2.0***	0.9	***0.0***	***0.0***	***1.8***
	24%	14%	0%	11%	11%	2%	10%	2%	4%	13%	10%	21%	0%	2%	40%
%	10%	36%	12%	20%	21%	0%	22%	14%	18%	2%	5%	8%	0%	5%	26%
	0%	0%	5%	10%	14%	11%	13%	7%	10%	17%	16%	10%	0%	0%	26%
W3	1.5	***2.1***	***0.0***	***2.2***	***0.3***	***0.4***	0.8	***0.3***	***0.6***	0.8	1.2	1.1	1.2	***1.9***	***1.5***
Ratio	1.1	***0.4***	1.2	0.8	1.1	1.2	***1.7***	0.7	***1.5***	0.8	***2.8***	1.0	***0.0***	***0.0***	0.2
	0.0	***0.3***	1.2	***1.8***	0.8	***0.4***	***1.7***	0.6	1.1	1.0	***0.0***	0.6	***0.2***	0.5	***2.7***
	17%	36%	0%	25%	4%	4%	8%	4%	10%	8%	13%	11%	12%	17%	36%
%	14%	12%	12%	8%	19%	14%	18%	5%	17%	6%	21%	13%	0%	0%	2%
	0%	2%	7%	14%	8%	4%	19%	6%	13%	19%	0%	10%	2%	5%	26%
W2	***0.0***	0.7	***0.0***	1.0	1.3	0.8	***0.1***	***0.3***	***2.1***	0.9	0.8	***2.6***	***2.5***	***3.4***	1.0
Ratio	***0.2***	0.8	1.0	***1.9***	1.2	***0.4***	***1.7***	***0.3***	***0.3***	***2.5***	***0.2***	***0.1***	***0.0***	***0.0***	0.2
	3.7	0.8	***5.0***	0.7	1.4	0.6	***2.4***	***0.6***	***0.5***	1.2	***0.0***	***0.6***	***0.3***	1.1	***0.3***
	0%	12%	0%	12%	14%	8%	1%	4%	33%	8%	8%	29%	26%	33%	21%
%	2%	19%	12%	17%	17%	6%	17%	3%	3%	21%	2%	2%	0%	0%	2%
	12%	7%	36%	6%	13%	7%	29%	5%	5%	22%	0%	10%	5%	10%	2%
W1	0.5	0.7	***0.0***	***1.6***	***1.7***	***0.0***	0.7	1.1	1.1	***2.8***	1.3	1.3	1.3	***2.2***	***1.6***
Ratio	***0.4***	***0.5***	1.9	***2.0***	0.9	***0.3***	1.2	1.3	***0.1***	***0.4***	***0.0***	0.6	***0.0***	***0.0***	1.0
	0.0	***2.0***	***3.0***	***2.1***	0.7	***0.4***	***1.6***	***1.4***	***0.5***	1.3	***0.0***	***0.6***	***0.3***	1.3	0.6
	5%	12%	0%	20%	17%	0%	7%	13%	15%	25%	13%	17%	14%	19%	36%
%	5%	12%	19%	18%	10%	5%	13%	10%	1%	3%	0%	8%	0%	0%	10%
	0%	24%	24%	20%	6%	5%	23%	13%	5%	24%	0%	10%	5%	12%	5%
O-D5	***0.3***	***0.0***	***0.0***	1.2	***0.6***	***0.0***	***1.5***	1.2	***0.5***	1.1	***0.5***	1.3	1.2	***0.4***	***2.0***
Ratio	***1.8***	0.6	***0.0***	1.0	***1.9***	***0.6***	0.7	1.0	***0.4***	***2.1***	0.7	1.0	***0.0***	***0.0***	0.7
	5.9	1.5	***1.7***	***1.4***	***2.4***	0.7	***1.5***	***1.5***	***0.6***	***1.5***	***0.0***	***0.5***	***0.2***	1.1	***2.3***
	3%	0%	0%	13%	7%	0%	16%	15%	6%	11%	4%	22%	13%	3%	43%
%	23%	10%	0%	10%	17%	8%	6%	8%	5%	13%	4%	11%	0%	0%	7%
	30%	17%	17%	15%	22%	8%	26%	11%	6%	24%	0%	9%	3%	13%	17%

favoured 2–3 weeks in advance of CAOs. The frequency of T4, T7, and T8 decreased after the CAO onset while an increase in T2 and T5 was evident.

During period 3 (P3), both a strong, off-centred PV pattern over the Beaufort Sea (T6) and weak PV patterns (T1 and T4) were favoured 3–4 weeks in advance of CAOs. High frequencies of weak PV patterns (T1 and T4) continued into Week 2 with a strong PV pattern increasing in frequency (T9). This suggests that 2–4 weeks in advance of P3 CAOs we might expect either a strengthening or weakening of the PV, however, weak PV patterns T1, T2, and T7 were favoured during Week 1 through the CAO onset. A clear consensus of preferred 100za patterns began to occur during week 2 of P3, with a stronger PV reducing in frequency near the onset in favour of a weak PV.

Similar to P3, period 4 (P4) experiences high frequencies of both strong PV and weak PV patterns. Transitional pattern T5 occurred most frequently during Week 3, while a strong PV pattern (T9) occurred most frequently during Weeks 2 and 4 and maintained a high, though not statistically significant, frequency of occurrence through the CAO onset. However, weak PV patterns T1, T4, and T7 began to increase in frequency 2 weeks before the CAO onset. Strong PV events centred over the Arctic are climatologically favoured near the end of the winter season; therefore, the relatively high frequency of strong PV events may be a result of the climatology of the pattern.

Period 5 (P5) is characterized by persistently strong PV patterns (T3, T6, and T9). An increase in weaker PV patterns (T7 and T8) was evident during Week 2 with T8 occurring 3.4 times as often as expected; however, Week 1 through the CAO onset once again favoured strong PV patterns (T3 and T9). While strong PV patterns were favoured throughout P5, the high frequency of occurrence of a PV off-centred towards North America (T3) indicates an increased likelihood of negative surface temperature anomalies in the eastern United States.

3.1.4 | SLP anomalies SOM

The ratio of each SLPa SOM pattern's occurrence preceding the CAO onset during each of the five periods is shown in Table 5. Though not significant, transitional pattern SLP5 and low-pressure pattern SLP6 occurred most frequently 2–4 weeks in advance of period 1 (P1) CAOs. By Week 1, North Atlantic blocking (SLP4) occurred nearly 3 times as often as expected. After the CAO onset, 87% of the patterns were weak PV and North Atlantic blocking patterns (SLP1, SLP4, and SLP7), which occurred 2–4 times as often as expected. Large variability across the North Atlantic was evident leading up to the CAO onset, with the Icelandic Low favoured 3–4 weeks in advance, transitioning to a strong North Atlantic high by the onset. Table 5 visually depicts this transition from the upper right portion of the SLPa SOM to the left side of the SOM.

Period 2 (P2) can most generally be characterized by the persistence of North Atlantic blocking. Much variability was present during Week 4 of P2 and only SLP5 occurred at a significant frequency above the climatologically expected. However, 3 weeks before the CAO through the onset favour a high frequency of positive anomalies over the Arctic and North Atlantic (SLP1, SLP2, and SLP4). Transitional pattern SLP5 decreased in frequency from Week 4 through Week 2 as strong North Atlantic blocking coupled with a weak PV (SLP1) became most favourable post-onset during P2.

A weak PV coupled with North Atlantic blocking (SLP1) continued as the preferred SOM pattern throughout period 3 (P3). Week 4 was characterized by high pattern variability, but 2–3 weeks before the CAO favoured an increase in weak PV and North Atlantic blocking patterns. By Week 1, SLP1 occurred 3.1 times more often than climatologically expected and accounted for 54% of all pattern occurrences compared with 18% expected. North Atlantic blocking remained twice as likely through Day 5 of the CAO, but slightly more variability began to occur with a small increase in low-pressure anomalies (SLP8).

Though a weak PV and North Atlantic blocking occurred most frequently throughout period 4 (P4), an increase in SLP variability was evident as higher frequencies of negative low-pressure anomalies in the Arctic (SLP8 and SLP9), indicative of a strong PV circulation, occurred 1–3 weeks before the CAO. However, Week 1 through the CAO onset still favoured a weak PV and North Atlantic blocking (SLP1 and SLP4), with SLP4 occurring 3.7 times more often than expected. A transition from high frequencies of occurrence of SLP1 (weakest PV centred over pole) to SLP4 (weak PV off-centred towards Greenland) post-onset may suggests a re-strengthening of the PV circulation, indicative of the high variability of SLP during P4.

Period 5 (P5) experienced a similar amount of pattern variability as P4 with a moderately strong PV (SLP8) favoured during Week 4 and a weaker PV favoured during Week 3 (SLP2). One to two weeks before the CAO favoured both North Atlantic blocking (SLP4 and SLP7) and the Icelandic Low (SLP6), with SLP7 occurring nearly 3 times as often as expected 2 weeks before the CAO and SLP4 occurring 2.6 times as often as expected 1 week before the CAO. North Atlantic blocking (SLP1, SLP4, and SLP7) continued to increase in frequency through the CAO onset, particularly SLP7 which occurred 4 times more often than expected from the onset through Day 5 of the CAO.

3.2 | Teleconnection influence on the synoptic patterns that drive CAOs

3.2.1 | Teleconnection indices compared with SOMs

Correlations between the AO, NAO, and PNA daily indices and the daily SOM patterns for each SOM variable reveals the largest correlations exist between the AO and NAO and

TABLE 5 (top) Ratios of SLPa pattern occurrences before CAOs and the climatologically expected occurrence. Blue shaded values indicate patterns which occur significantly more frequently prior to CAOs than climatologically expected, while red shaded values occur significantly less frequently prior to CAOs. Bold italic values are statistically significant, where dark blue and dark red are statistically significant at the 95% confidence level while light blue and light red are statistically significant at 90% confidence level. (Bottom) Percentage of occurrence of each pattern. Columns represent each of the five periods (P1–P5). Rows represent weeks before onset (W1–W4) and onset—day 5 of the CAO (O–D5)

Ratio	P1			P2			P3			P4			P5		
W4 Ratio	1.0	0.8	0.9	1.0	0.7	1.1	***1.4***	***0.4***	***0.3***	***1.5***	1.4	1.3	***0.0***	***1.9***	0.7
	1.1	***1.5***	1.5	0.9	***1.8***	1.0	0.9	0.8	***1.6***	0.7	***0.4***	***0.2***	1.3	0.9	1.7
	1.7	***0.2***	***0.0***	0.9	0.7	1.1	1.2	***2.1***	***0.3***	***1.5***	0.7	***0.4***	1.0	0.7	0.9
%	10%	10%	10%	11%	7%	12%	15%	4%	4%	22%	13%	16%	0%	19%	10%
	12%	26%	19%	11%	19%	10%	9%	8%	19%	6%	3%	2%	12%	10%	14%
	12%	2%	0%	10%	8%	13%	17%	21%	4%	27%	6%	5%	17%	7%	12%
W3 Ratio	0.7	1.1	1.3	0.8	0.8	***0.6***	1.1	0.3	0.4	1.1	***0.0***	***1.6***	***0.3***	1.0	0.6
	1.1	1.2	0.5	1.0	***1.7***	***0.2***	1.6	0.8	0.7	***2.0***	***1.8***	1.0	1.6	1.3	0.9
	0.7	1.0	1.1	***1.7***	***1.4***	0.6	1.6	1.6	1.0	***0.3***	***0.3***	1.3	***0.5***	***1.6***	1.5
%	7%	14%	17%	10%	7%	7%	13%	3%	6%	14%	0%	17%	2%	10%	10%
	12%	19%	7%	12%	18%	2%	13%	7%	9%	21%	14%	8%	14%	12%	10%
	5%	10%	10%	23%	14%	7%	24%	15%	11%	6%	3%	16%	7%	17%	19%
W2 Ratio	1.3	0.7	1.1	1.3	1.3	1.3	***0.2***	0.9	***0.7***	1.2	***1.8***	1.1	***2.9***	0.9	0.6
	0.7	1.4	2.4	***1.4***	***0.2***	0.7	1.1	1.0	0.8	***1.5***	0.6	0.8	0.9	0.7	2.4
	0.0	***0.4***	***0.3***	0.7	1.3	***0.6***	***2.1***	1.3	0.8	***1.6***	***0.3***	***0.2***	***0.1***	0.5	***0.7***
%	12%	10%	14%	17%	12%	18%	3%	9%	10%	13%	13%	13%	29%	10%	10%
	7%	21%	29%	17%	2%	7%	9%	8%	8%	16%	5%	6%	7%	7%	24%
	0%	5%	2%	8%	13%	6%	33%	12%	9%	29%	3%	3%	2%	5%	7%
W1 Ratio	1.3	1.2	0.7	1.4	***0.5***	***0.2***	0.8	0.9	***0.3***	0.9	0.9	***1.5***	0.5	0.8	0.9
	2.8	1.1	0.2	***2.4***	1.3	0.7	0.7	0.7	***0.2***	1.1	***0.3***	0.7	***2.6***	0.6	2.4
	1.3	***0.2***	***0.2***	***1.4***	0.8	***0.2***	***3.1***	***0.5***	***0.3***	***2.1***	***0.5***	***0.2***	0.9	***0.0***	0.5
%	12%	14%	7%	17%	5%	2%	12%	9%	4%	8%	6%	17%	5%	10%	14%
	31%	17%	2%	27%	14%	7%	6%	5%	2%	13%	3%	6%	26%	5%	21%
	12%	2%	2%	17%	8%	2%	54%	4%	4%	37%	6%	3%	14%	0%	5%
O-D5 Ratio	***2.0***	***0.0***	***0.0***	0.9	1.0	***0.0***	1.2	***1.5***	***0.3***	1.1	***1.6***	***0.3***	***4.0***	***0.3***	0.8
	2.2	***0.0***	***0.3***	1.1	1.2	***0.0***	0.8	1.2	***0.0***	***3.7***	0.9	***0.0***	***2.7***	0.4	***0.0***
	3.7	1.0	***0.0***	***2.7***	***1.6***	***0.3***	***2.0***	0.7	***0.3***	***1.5***	***0.2***	***0.0***	1.1	***0.0***	***0.0***
%	23%	0%	0%	10%	10%	0%	19%	14%	4%	9%	13%	4%	37%	3%	13%
	27%	0%	3%	12%	12%	0%	8%	9%	0%	38%	9%	0%	27%	3%	0%
	37%	10%	0%	37%	17%	3%	38%	6%	4%	24%	2%	0%	17%	0%	0%

TABLE 6 Correlation between AO, NAO, and PNA (left column) indices and the SOM variables (top row). Bold values are statistically significant with $p < .05$

	SLPa			100za			10za		
AO	***-0.01***	***0.22***	***0.41***	***-0.03***	***0.13***	***0.30***	***-0.11***	***-0.07***	***-0.03***
	-0.14	***0.11***	***0.18***	***-0.13***	***0.02***	***0.13***	***-0.02***	***-0.04***	0.01
	-0.51	***-0.16***	***-0.07***	***-0.32***	***-0.13***	***-0.01***	***0.07***	***0.07***	***0.10***
NAO	***-0.12***	***0.05***	***0.21***	***-0.17***	0.01	***0.21***	***-0.04***	0.00	***0.05***
	-0.16	***0.09***	***0.17***	***-0.15***	0.02	***0.13***	***-0.10***	***-0.08***	***0.03***
	-0.29	-0.02	***0.07***	***-0.17***	-0.01	***0.12***	0.01	***0.02***	***0.12***
PNA	0.01	***0.04***	***0.08***	***0.08***	***0.09***	0.02	***0.04***	***-0.03***	***-0.10***
	-0.03	***-0.03***	-0.01	***0.05***	0.02	***-0.09***	0.02	***-0.05***	***-0.02***
	-0.06	0.00	***0.01***	0.01	***-0.04***	***-0.14***	***0.06***	***0.05***	***0.03***

the SLPa and 100za patterns, particularly for the extreme SLPa patterns such as SLP1 and SLP9 (Table 6). There is relatively no correlation between the SOM variable patterns and the PNA. The 10za patterns also correlate poorly with the AO, NAO, and PNA. The relationship between the SOM variables and teleconnections was expected since SLP is a surface variable as opposed to the 100z and 10z anomalies and demonstrates the SLP anomalies were the most appropriate variable near the CAO onset. The AO had the highest correlation of the three teleconnections because the SOM's spatial extent focused on the north pole (45°–90°N). The southern pole of the NAO dipole, a semi-permanent region of high pressure near the Azores, and the two southernmost poles in the PNA quadripole, were outside of the SOM's spatial extent, therefore had a lower correlation with the SOM patterns.

The daily teleconnection indices were composited for each SOM pattern (Table 7). The most extreme positive and negative values were evident in the AO composites, specifically the 100z and SLP composite. The values were closer to neutral for the NAO composites and near neutral for the PNA composite, further suggesting that the relationship was weaker between SOM nodes and these teleconnections. The 10z anomalies do not correlate well with the AO, NAO, or PNA because there is a time lag between an atmospheric pattern materializing at 10 mb and its effects at the surface, whereas the SLP values are a measurement of the surface conditions, and therefore have the highest correlations to the AO and NAO. Nonetheless, the average indices do align well with the expected SOM patterns, with negative AO values in the lower left of the SLP and 100za SOM and the upper left for the 10z anomalies SOM. The positive AO

TABLE 7 Average AO, NAO, and SLP teleconnection indices for 10z, 100z, and SLP for each SOM pattern

	10z			100z			SLP		
AO	-0.73	-0.64	-0.35	-0.33	0.43	1.18	-0.23	0.95	1.62
	-0.28	-0.34	-0.14	-0.88	-0.10	0.48	-0.94	0.36	0.76
	0.14	0.18	0.27	-1.75	-0.91	-0.25	-2.41	-1.04	-0.58
NAO	-0.02	0.07	0.19	-0.33	0.10	0.52	-0.21	0.20	0.51
	-0.17	-0.07	0.14	-0.29	0.12	0.37	-0.31	0.28	0.48
	0.08	0.12	0.31	-0.30	0.05	0.36	-0.52	0.03	0.25
PNA	0.14	-0.03	-0.19	0.23	0.25	0.09	0.07	0.14	0.21
	0.11	-0.03	0.00	0.17	0.11	-0.16	-0.01	-0.02	0.04
	0.18	0.17	0.12	0.08	-0.05	-0.31	-0.07	0.06	0.09

values are focused on the upper right portion of the SOM for SLP and 100z and the lower portion of the SOM for 10z. The NAO is similar to the AO, but the negative values are focused on the left and transition to positive values on the right of the 100z and SLP SOMs as opposed to a diagonal transition from the lower left to the upper right. While the 10z anomalies do not correlate well with the NAO, positive values do favour the right side. The PNA, being a quadripole of pressure centres, contains more noise than both the AO and NAO and is poorly represented by both the 10z and SLP anomalies. The composite of the PNA with the 100z anomaly SOM maintains the best separation in values with positive indices in the upper left and negative indices in the lower right.

3.2.2 | Daily teleconnection indices impacts on CAOs

The 67-year average teleconnection indices for each day of the winter season (October–March) smoothed with a sixth-order polynomial regression, are shown in Figure S1, Supporting Information. Each index favours a near-neutral phase during early and late winter. The AO trends negative throughout mid-winter; however, the NAO and PNA trend slightly positive throughout the winter. Therefore, a negative AO is favoured during mid-winter while a positive NAO and PNA are increasingly favoured throughout the winter. The amplitude of the polynomial regressions also indicates the amount of variability throughout the winter season, with the AO and NAO being most variable and the PNA being the least variable.

The average teleconnection indices leading up to the CAO onset for P1–P5 are shown in Table 8. A negative AO is favoured post-CAO onset for all periods while a negative NAO is favoured post-CAO onset during P1 through P3, but is near neutral during P4 and P5 CAOs. The AO and NAO both exhibit more persistently negative phases leading up to the CAO onset during mid-winter CAOs (P2–P4) with the most persistently negative values having occurred during P3. The AO favours a strongly negative phase near the CAO onset through Day 5 during all five periods, however, the AO is much more variable during the weeks leading up to P1 and P5 CAOs as opposed to P2, P3, and P4 CAOs. This suggests that P1 and P5 CAOs are characterized by a rapid weakening of the PV as it transitions to a negative phase AO, whereas P2, P3, and P4 CAOs favour a persistently weak PV. This is also evident during P1 and to a lesser extent P5 for the NAO. The near-neutral NAO is favoured leading up to the CAO onset during P1 and through the CAO onset during P5. The PNA is less consistent with both positive and negative patterns occurring through each period leading up to CAOs. P2, and P3 have the most persistently positive average PNA phase, while P1, particularly near the CAO onset, favours a negative PNA phase. When compared with the 67-year average teleconnection indices, the observed strongly negative AO values are not expected

TABLE 8 Daily average teleconnection indices by period 4 weeks prior to the CAO onset through Day 5 of the CAO. (top) AO, (middle) NAO, (bottom) PNA. Red highlights indices favouring above average temperatures in the eastern United States, while blue highlights indices favouring below average temperatures in the eastern United States. Italic bold values are statistically significant with $p < .05$ and bold values are statistically significant with $p < .10$

AO	W4	W3	W2	W1	O - D5	Avg.
P1	-0.19	0.07	***0.60***	***-0.48***	***-1.60***	-0.32
P2	***-0.42***	***-0.77***	-0.18	***-0.35***	***-1.31***	-0.61
P3	***-0.70***	***-1.28***	***-1.28***	***-1.70***	***-1.46***	-1.29
P4	***-0.78***	-0.31	***-0.80***	-0.48	***-0.86***	-0.65
P5	-0.44	-0.69	***0.38***	**0.12**	***-1.29***	-0.39
Avg.	-0.50	-0.59	-0.26	-0.58	-1.30	
NAO						
P1	0.01	0.00	***0.29***	***0.33***	***-0.43***	0.04
P2	**-0.12**	***-0.35***	-0.03	***-0.25***	***-0.76***	-0.30
P3	***-0.28***	***-0.48***	***-0.36***	***-0.49***	***-0.53***	-0.43
P4	***-0.19***	**-0.10**	***-0.41***	***-0.24***	***-0.05***	-0.20
P5	0.14	0.14	0.17	0.27	**0.01**	0.14
Avg.	-0.09	-0.16	-0.07	-0.07	-0.35	
PNA						
P1	***0.45***	-0.04	***-0.64***	***-0.57***	***-0.30***	-0.22
P2	**-0.16**	**-0.15**	***0.28***	**0.14**	0.02	0.02
P3	***-0.11***	0.13	***0.20***	**0.09**	***0.24***	0.11
P4	***0.30***	***0.21***	***-0.04***	***-0.05***	0.08	0.10
P5	0.14	0.28	-0.01	***-0.19***	***-0.28***	-0.01
Avg.	0.12	0.09	-0.04	-0.12	-0.05	

during P1 and P2, or late in P5. Like the AO, the observed negative NAO indices during P2 through P4 would not be expected. The PNA, having less variability according to the 67-year average, is much closer to the expected values throughout each period.

The difference between the daily mean composite teleconnection indices (Table 8) and the 67-year mean teleconnection indices (Figure S1) by period are shown in Table 9. For both the AO and the NAO, the indices after the CAO onset through Day 5 of the CAO (O–D5) favoured a much lower than expected value. Both the AO and NAO favour indices lower than expected during the entire period leading up to mid-winter CAOs (P2–P4), particularly the AO during P3. The PNA favours lower than normal values preceding early and late winter CAOs and near-normal to above normal values preceding mid-winter CAOs. The below-normal PNA indices during early and late winter would suggest a favouring of a warm pattern in the eastern United States. During P1, both the NAO and PNA favour a warm pattern in the eastern United States, however, by the CAO onset, the AO and NAO favour much lower than normal indices. This

TABLE 9 The difference between the daily average composite teleconnection indices (Table 8) and the 67-year average teleconnection indices (Figure S1) by period. Blue indicates a difference that favours a colder pattern in the eastern United States. Red indicates a difference that favours a warmer pattern in the eastern United States. Italic bold values are statistically significant with $p < .05$ and bold values are statistically significant with $p < .10$

AO	W4	W3	W2	W1	O - D5
P1	-0.19	0.12	***0.58***	***-0.50***	***-1.54***
P2	***-0.43***	***-0.72***	-0.21	***-0.38***	***-1.25***
P3	***-0.70***	***-1.24***	***-1.31***	***-1.73***	***-1.40***
P4	***-0.79***	-0.26	***-0.83***	***-0.51***	***-0.80***
P5	**-0.45**	***-0.65***	0.35	0.10	***-1.23***
NAO	W4	W3	W2	W1	O - D5
P1	0.09	**0.10**	***0.35***	***0.36***	***-0.46***
P2	-0.04	**-0.24**	0.03	-0.22	***-0.79***
P3	-0.20	***-0.37***	**-0.30**	***-0.46***	***-0.56***
P4	-0.11	0.00	***-0.35***	**-0.21**	-0.09
P5	***0.22***	***0.24***	***0.24***	***0.29***	-0.02
PNA	W4	W3	W2	W1	O - D5
P1	***0.44***	-0.10	***-0.66***	***-0.60***	***-0.31***
P2	***-0.17***	***-0.21***	***0.27***	0.12	0.01
P3	-0.13	0.07	***0.19***	0.07	***0.23***
P4	***0.29***	0.15	-0.05	-0.07	0.07
P5	0.13	0.22	-0.02	**-0.21**	***-0.28***

suggests that early winter CAOs, and late winter CAOs to some degree, are characterized by a sudden onset of favourable CAO conditions, whereas mid-winter CAOs are preceded by persistently favourable conditions.

4 | DISCUSSION

The variables used in this study represent conditions at the surface (SLPa), the upper troposphere (100za), and the stratosphere (10za), thus provide a multi-level approach to characterize the evolution of patterns associated with CAOs. Because of the proximity to the surface, SLPa patterns are a direct representation of surface conditions and fluctuate more than 100za patterns, which fluctuate more than the 10za patterns. The lower-frequency pattern variability of the 10za and 100za SOM patterns and their lagged response with the surface make them a useful forecasting tool as anomalous patterns may manifest in the upper troposphere or stratosphere weeks before the surface effects materialize. This relationship has been noted by Cohen and Jones (2011) who showed weak tropospheric PV events are often preceded by weak stratospheric PV events and Kolstad *et al.* (2010) who further suggested the coupling between the stratospheric weak PV events and the troposphere could be used to enhance medium range and seasonal forecasts. For this reason, the SLPa SOM is most applicable 1–2 weeks before the CAO onset through Day 5 of the CAO, while the 10za and 100za SOMs provide the clearest insight 1–4 weeks prior to the onset. Thus, the 10za and 100za SOM patterns are best viewed in terms of their potential impacts on lower levels of the atmosphere and should not be considered as direct representations of surface weather.

The SLPa SOM patterns favour a weak PV with North Atlantic blocking during the 2 weeks leading up to a CAO during all five periods, previously noted by Cellitti *et al.* (2006). Similar to the findings of Baldwin and Dunkerton (2001), this study found persistent circulation anomalies in the stratosphere (10za) favoured tropospheric (100za) anomalies of the same sign. Both the 10za and 100za SOM patterns revealed a strong and/or off-centred PV was favoured three to 4 weeks in advance of late season CAOs (P4 and P5), consistent with the findings of Seviour *et al.* (2013), and a weak PV was favoured prior to mid-winter CAOs (P2 and P3). This relationship between a weak stratospheric PV and CAOs has been observed in several studies: Kidston *et al.* (2015) determined there was a higher likelihood of extremely low-temperature over the eastern United States following a weakening of the stratospheric jet; Kolstad *et al.* (2010) showed the probability of CAOs increased by more than 50% in Europe, Asia, and eastern North America following a weak stratospheric PV; and Thompson *et al.* (2002) found a weakened stratospheric PV was typically followed by episodes of anomalously low surface air temperatures and an increase in frequency of persistent extreme cold events in eastern North America, northern Europe, and eastern Asia. While a strong, off-centred PV transitioned to a predominantly weak PV during P4, P1 CAOs favoured a weak PV (tropospheric and stratospheric) 3–4 weeks prior to the CAO onset transitioning to a predominantly strong, off-centred PV 1 week before the onset. This confirms that while a weak tropospheric and stratospheric PV is favourable for negative SLP anomalies across the Arctic and North Atlantic throughout much of winter, they may also be preceded by a strong PV in the troposphere and stratosphere. However, the negative SLP anomalies during P1 and P4 may be less attributed to the phase of the PV and more so to the fluctuations of the PV. A rapid transition from a weak PV to a strong PV (P1) or a strong PV to a weak PV (P4) in the stratosphere may have prompted an anomalous Rossby wave pattern at the surface, resulting in negative SLP anomalies in the Arctic and North Atlantic. The development of a strong PV near the CAO onset during P1 may also be attributed to the anomalous surface temperatures across eastern North America strengthening the PV circulation (Cellitti *et al.*, 2006). Inconsistencies of the PV strength preceding CAOs further support the need to incorporate other high variability surface circulations, such as the AO, NAO, and PNA, alongside the PV when forecasting CAOs.

The teleconnection analysis reveals negative values of the NAO and AO occur commonly prior to North American CAOs, consistent with the findings of both Cellitti *et al*. (2006) and Walsh *et al*. (2001). A negative NAO, particularly when coupled with a negative AO, is indicative of North Atlantic blocking which favours the channelling of Arctic air into the eastern United States by causing a trough to form east of the Rocky Mountains (Westby and Black, 2015). This is evident in the SLPa SOM with negative anomalies across the Arctic and North Atlantic 1–2 weeks prior to the CAO onset. There is a clear relationship between the persistently weak tropospheric and stratospheric PV during mid-winter CAOs (P2 and P3) and the negative AO and NAO indices during P2, P3, and P4. These results align well with Kolstad *et al*. (2010) who showed that the stratosphere can influence the troposphere via the AO and Woollings *et al*. (2010) who found an increase in high-latitude blocking events during SSW events. The PNA also favours positive indices during the core of winter (P2–P4) increasing the likelihood of a ridge in the western United States with a trough in the eastern United States. Early and late season CAOs, which favour more variability in the PV, experience less persistence in the AO. This is evident in the daily AO indices as a rapid change to a negative AO phase occurs near the CAO onset during P1 and P5. The NAO also favours a rapid transition to a negative phase during P1, along with predominantly negative indices during P2, P3, and P4. However, the NAO is predominantly positive during P5, likely the result of a positive NAO climatologically favoured during late winter.

The findings of this research are similar to other studies in that a persistently weak tropospheric (100za) and/or stratospheric (10za) PV exists shortly prior to the CAO onset (Cellitti *et al*., 2006); however, this study also shows that the PV has some level of CAO predictability as much as 28 days in advance of most CAOs, particularly during mid-winter (P2 and P3). Negative phases of the AO and NAO are evident during periods with a weak PV, favouring a weakening of the zonal winds across North America, thus a southwards displacement of Arctic air in the eastern United States. Though weak PV patterns are favoured prior to CAOs, this research finds that when high frequencies of strong PV patterns precede CAOs (P1, P4, and P5), three inferences can be made:

1. The strong PV is off-centred towards North America, favouring negative surface temperature anomalies in the eastern United States.
2. The transition of a weak PV 3–4 weeks in advance of the CAO to a strong PV near the onset may be a manifestation of the negative surface temperature anomalies in the upper atmosphere.
3. Predominantly strong PV patterns 3–4 weeks in advance of the CAO transitioning to predominantly weak PV patterns 1–2 weeks prior to the CAO onset may indicate rapid weakening of the PV, which materialize at the surface shortly after.

The incongruencies between variables, particularly between the upper level (10za and 100za) and surface (SLPa) SOMs, were a result of the multi-level analysis used in this study. While the 10za and 100za SOMs were similar in that they favoured a stronger, off-centred PV during early and late winter CAOs, the SLPa SOM suggests the opposite (negative Arctic and North Atlantic anomalies). This indicates that the conditions favourable for early and late winter CAOs may develop sooner to the onset or the relationship between the stratospheric and tropospheric PV and other variables contributing to the CAO behave differently preceding mid-winter CAOs. Additionally, the 10za and 100za SOM patterns are biased to the climatologically expected patterns 3–4 weeks prior to early and late winter CAOs, suggesting SLP anomalies, while providing less lead time, are the most applicable variable prior to early and late winter CAOs.

5 | CONCLUSION

Extreme weather occurs relatively infrequently throughout the year, yet it is the extreme events that impact people and the economy the most. Cold air outbreaks (CAOs) are one form of extreme weather that affects regions in the mid-latitudes during the winter and may result in crop loss, excessive energy consumption, and even death. Though vast improvements in forecasting have been made over recent decades, necessary preparations for extreme events often require longer lead times than can be acquired from dynamical models. Early season extreme cold has been shown to increase the relative risk of mortality across the United States (Smith and Sheridan, 2018a,b); thus, increased predictability of early season CAOs could potentially limit the aforementioned risk of increased mortality. This research has shown the continuous pattern representation of SLP, 10z, and 100z anomalies with SOMs provides key benefits when working with continuous data and allows for a systematic identification of patterns that commonly lead to CAOs. This study builds upon previous literature in that it directly addresses the temporal relationship between a weakened PV and resultant CAO, while further contextualizing the relationship of upper and lower atmospheric variables prior to the CAO. Moreover, this study demonstrates the PV has potential to be a useful advanced predictor for CAOs, but the lack of a consistent signal between the PV and SLP prior to early and late season CAOs in the eastern United States suggests further studies are needed to better understand the temporal inconsistencies.

SLP anomalies, if considered within 2 weeks of the CAO, present the most consistent synoptic patterns preceding CAOs in the eastern United States, while the lag between upper atmospheric anomalies and the surface manifestation makes the 10z and 100z anomalies most applicable 1–4 weeks prior to the CAO. It is this lag between the upper stratosphere (10z), upper troposphere (100z), and the surface (SLP) that increase CAO predictability beyond the range of dynamical models. Negative SLP anomalies across the Arctic and North Atlantic are evident during the 2 weeks before a CAO onset through Day 5 of the CAO for all five periods, indicative of a weak PV and negative NAO. The 10za and 100za SOM patterns reveal a strong, off-centred stratospheric and tropospheric PV over North America is favoured prior to early and late winter CAOs (P1 and P5). A weak stratospheric and tropospheric PV occurs most frequently preceding mid-winter CAOs (P2–P4). Though not as persistent, a weak PV is also evident prior to early and late winter CAOs (P1 and P5). Thus, 37 of the 49 CAOs favour persistently weak PV patterns prior to onset, while the remaining 12 CAOs favour either a strong tropospheric or stratospheric PV off-centred towards North America or a strong PV transitioning to a weak PV near the onset. Mid-winter CAOs (P2–P4) favoured a persistently negative AO and NAO during the 28 days leading up to the CAO through Day 5. While a sharply negative phase AO was favoured during CAOs for all five periods, early and late winter CAOs (P1 and P5) experienced a higher frequency of neutral and positive AO phases prior to the CAO. This coincides well with the negative Arctic SLP anomalies throughout all five periods of the winter. Similarly, early and late winter CAOs were preceded by higher frequencies of neutral and positive NAO phases. The results of the PNA were less clear than the AO and NAO; however, a neutral to positive phase PNA was favoured prior to P3 CAOs. The lack of a negative phase NAO during late season CAOs is indicative of the predominantly strong, off-centred PV over North America; thus a negative phase NAO is not necessary to direct cold air into the eastern United States when the PV is already displaced towards North America. This study concludes that CAOs in the eastern United States are immediately preceded by negative SLP anomalies across the Arctic and North Atlantic regardless of the time of the winter, as seen by the negative phase AO. Therefore, a negative AO phase, often coupled with a negative NAO phase, increases the likelihood of eastern U.S. CAOs within 1–2 weeks. Furthermore, the tropospheric PV anomalies closely resemble the stratospheric PV anomalies, suggesting the likelihood of CAOs increases 2–4 weeks after the weakening of a stratospheric PV, particularly from late November through late February, whereas the inconsistency of the strength of the PV prior to early and late season CAOs suggests that the transition to and from meteorological winter may result in a lowered predictability of CAOs. As noted by Kolstad *et al*. (2010), the lack of a consistent PV signal limits the usefulness of the PV as a predictor, thus more research should be conducted to delineate the relationship of the PV with early and late season CAOs in the eastern United States.

The knowledge of the atmospheric precursors to CAOs is still imperfect and much more research needs to be done to advance the understanding. This study focused on the influence of the PV on a narrow region in the mid-latitudes; however, expanding the study area to the entire mid-latitudes of the Northern Hemisphere would be beneficial. Future research will utilize a similar synoptic classification via SOMs, but instead of surface station data, reanalysis data will be used to define CAOs. This will provide a more holistic approach to understanding the characteristics of the PV preceding CAOs across the globe. Continued exploration of the effect specific teleconnections has on the magnitude, duration, and location of Arctic air displacement is also necessary. Future studies will also focus on a more in-depth analysis of how the PV behaves prior to early, mid, and late season CAOs to better understand the inconsistencies the PV exhibited in this study.

ORCID

Erik T. Smith https://orcid.org/0000-0002-8133-0348

REFERENCES

Baldwin, M.P. and Dunkerton, T.J. (2001) Stratospheric harbingers of anomalous weather regimes. *Science*, 294(5542), 581–584.

Cassano, J.J., Uotila, P. and Lynch, A. (2006) Changes in synoptic weather patterns in the polar regions in the twentieth and twenty-first centuries, part 1: Arctic. *International Journal of Climatology*, 26(8), 1027–1049.

Cellitti, M.P., Walsh, J.E., Rauber, R.M. and Portis, D.H. (2006) Extreme cold air outbreaks over the United States, the polar vortex, and the large-scale circulation. *Journal of Geophysical Research: Atmospheres*, 111(D2), D02114.

Cohen, J. and Jones, J. (2011) Tropospheric precursors and stratospheric warmings. *Journal of Climate*, 24, 6562–6572.

Deser, C. (2000) On the teleconnectivity of the "Arctic Oscillation". *Geophysical Research Letters*, 27(6), 779–782.

Gibson, P.B., Uotila, P., Perkins-Kirkpatrick, S.E., Alexander, L.V. and Pitman, A.J. (2016) Evaluating synoptic systems in the CMIP5 climate models over the Australian region. *Climate Dynamics*, 47(7–8), 2235–2251.

Griffiths, M.L. and Bradley, R.S. (2007) Variations of twentieth-century temperature and precipitation extreme indicators in the northeast United States. *Journal of Climate*, 20(21), 5401–5417.

Huth, R., Beck, C., Philipp, A., Demuzere, M., Ustrnul, Z., Cahynová, M., Kyselý, J. and Tveito, O.E. (2008) Classifications of atmospheric circulation patterns. *Annals of the New York Academy of Sciences*, 1146(1), 105–152.

Johnson, N.C., Feldstein, S.B. and Tremblay, B. (2008) The continuum of Northern Hemisphere teleconnection patterns and a description of the NAO shift with the use of self-organizing maps. *Journal of Climate*, 21(23), 6354–6371.

Kalnay, E., Kanamitsu, M., Kistler, R., Collins, W., Deaven, D., Gandin, L., Iredell, M., Saha, S., White, G., Woollen, J. and Zhu, Y. (1996) The NCEP/NCAR 40-year reanalysis project. *Bulletin of the American Meteorological Society*, 77(3), 437–472.

Kidston, J., Scaife, A.A., Hardiman, S.C., Mitchell, D.M., Butchart, N., Baldwin, M. P. and Gray, L. J. (2015) Stratospheric influence on tropospheric jet streams, storm tracks and surface weather. *Nature Geoscience*, 8(6), 433.

Kohonen, T. (2013) Essentials of the Self-Organizing Map. *Neural Networks*, 37, 52–65. https://doi.org/10.1016/j.neunet.2012.09.018.

Kolstad, E.W., Breiteig, T. and Scaife, A.A. (2010) The association between stratospheric weak polar vortex events and cold air outbreaks in the Northern Hemisphere. *Quarterly Journal of the Royal Meteorological Society*, 136(649), 886–893.

Mitchell, D.M., Gray, L.J., Anstey, J., Baldwin, M.P. and Charlton-Perez, A.J. (2013) The influence of stratospheric vortex displacements and splits on surface climate. *Journal of Climate*, 26(8), 2668–2682.

Ning, L. and Bradley, R.S. (2014) Winter precipitation variability and corresponding teleconnections over the northeastern United States. *Journal of Geophysical Research: Atmospheres*, 119(13), 7931–7945.

Ott, L. (1977) Categorical data. In: *Introduction to Statistical Methods and Data Analysis*. North Scituate, MA: N. Pag. Print.

Pinto, J.G., Reyers, M. and Ulbrich, U. (2011) The variable link between PNA and NAO in observations and in multi-century CGCM simulations. *Climate Dynamics*, 36(1–2), 337–354.

Seviour, W.J.M., Mitchell, D.M. and Gray, L.J. (2013) A practical method to identify displaced and split stratospheric polar vortex events. *Geophysical Research Letters*, 40(19), 5268–273.

Sheridan, S.C. and Lee, C.C. (2011) The self-organizing map in synoptic climatological research. *Progress in Physical Geography*, 35(1), 109–119.

Smith, E.T. and Sheridan, S.C. (2018a) The characteristics of extreme cold events and cold air outbreaks in the eastern United States. *International Journal of Climatology*, 38, e807–e820.

Smith, E.T. and Sheridan, S.C. (2018b) The influence of extreme cold events on mortality in the United States. *Science of the Total Environment*, 647, 342–351.

Thompson, D.W., Baldwin, M.P. and Wallace, J.M. (2002) Stratospheric connection to Northern Hemisphere wintertime weather: Implications for prediction. *Journal of Climate*, 15(12), 1421–1428.

Thompson, D.W.J. and Wallace, J.M. (1998) The Arctic Oscillation signature in the wintertime geopotential height and temperature fields. *Geophysical Research Letters*, 25(9), 1297–1300.

Vavrus, S., Walsh, J.E., Chapman, W.L. and Portis, D. (2006) The behavior of extreme cold air outbreaks under greenhouse warming. *International Journal of Climatology*, 26(9), 1133–1147.

Wallace, J.M. and Gutzler, D.S. (1981) Teleconnections in the geopotential height field during the Northern Hemisphere winter. *Monthly Weather Review*, 109(4), 784–812.

Walsh, J.E., Phillips, A.S., Portis, D.H. and Chapman, W.L. (2001) Extreme cold outbreaks in the United States and Europe, 1948–99. *Journal of Climate*, 14(12), 2642–2658.

Waugh, D.W., Sobel, A.H. and Polvani, L.M. (2017) What is the polar vortex and how does it influence weather? *Bulletin of the American Meteorological Society*, 98(1), 37–44.

Westby, R.M. and Black, R.X. (2015) Development of anomalous temperature regimes over the southeastern U.S.: synoptic behavior and role of low-frequency modes. *Weather and Forecasting*, 30(3), 553–570.

Wettstein, J.J. and Mearns, L.O. (2002) The influence of the North Atlantic–Arctic Oscillation on mean, variance, and extremes of temperature in the northeastern United States and Canada. *Journal of Climate*, 15(24), 3586–3600.

Wheeler, D.D., Harvey, V.L., Atkinson, D.E., Collins, R.L. and Mills, M.J. (2011) A climatology of cold air outbreaks over North America: WACCM and ERA-40 comparison and analysis. *Journal of Geophysical Research: Atmospheres*, 116(D12), D12107.

Woollings, T., Hannachi, A. and Hoskins, B. (2010) Variability of the North Atlantic eddy-driven jet stream. *Quarterly Journal of the Royal Meteorological Society*, 136(649), 856–868.

SUPPORTING INFORMATION

Additional supporting information may be found online in the Supporting Information section at the end of the article.

How to cite this article: Smith ET, Sheridan SC. The influence of atmospheric circulation patterns on cold air outbreaks in the eastern United States. *Int J Climatol*. 2019;39:2080–2095. https://doi.org/10.1002/joc.5935